Available online at www.sciencedirect.com
SCIENCE DIRECT®
Thin Solid Films 436 (2003) 175–180
thin solid films
www.elsevier.com/locate/tsf

Deposition and properties of CBD and CSS CdS thin films for solar cell application

H.R. Moutinho*, D. Albin, Y. Yan, R.G. Dhere, X. Li, C. Perkins, C.-S. Jiang, B. To, M.M. Al-Jassim

National Renewable Energy Laboratory, 1617 Cole Blvd, Golden, CO 80401, USA

Received 16 October 2002; received in revised form 20 March 2003; accepted 14 April 2003

Abstract

We deposited cadmium sulfide (CdS) thin films using the chemical-bath deposition (CBD) and close-spaced sublimation (CSS) techniques. The films were then treated in $CdCl_2$ vapor at 400 °C for 5 min. The CSS CdS films had hexagonal structure, and good crystallinity. The $CdCl_2$ treatment did not produce major changes, but there was a decrease in the density of planar defects. The untreated CBD CdS films had cubic structure and poorer crystallinity than the CSS films. After the $CdCl_2$ treatment, these films recrystallized to the hexagonal phase, resulting in better crystallinity and a lower density of planar defects. The conformal coverage and the presence of bulk oxygen are the key issues in making the CBD films more suitable for photovoltaic applications.

Keywords: Cadmium sulfide; Close-spaced sublimation; Chemical-bath deposition

1. Introduction

CdS, with its large bandgap and chemical stability, is an n-type semiconductor used as a window layer in many types of solar cells in conjunction with absorbers such as $Cu(In_{1-x}Ga_x)Se_2$ [1] and CdTe [2]. The best cell efficiencies attained so far are 16.5% [3] (CdTe/CdS) and 21.5% [4] and 18.8% [5] (CIGS/CdS, with and without concentration, respectively). In these devices, the light penetrates the CdS layer and is absorbed in the p-type semiconductor close to the pn-junction. Light absorbed in the CdS layer in general decreases the quantum efficiency in the blue part of the spectrum [6], and should be avoided. To minimize this loss, the CdS is made as thin as possible. At present, the CdS used in solar cells is usually deposited by CBD [7]. Nevertheless, this technique is cumbersome and not appropriate for large-scale production of solar cells. For these reasons, other techniques for depositing CdS are being investigated [8,9]. In this work, we compare CdS films grown using the standard CBD technique and films grown by CSS, and explain why cells made with the former technique generally have better efficiencies. Finally, we will report on the effects of the $CdCl_2$ treatment on the properties of the CdS films. This treatment has been shown as an important step in the processing of CdS and other semiconductors used in photovoltaic devices [10–12].

2. Experimental procedure

The films were grown on two types of substrates: SnO_2/borosilicate glass and SnO_2/Si. The former substrate structure is the one used in CdTe/CdS solar cells, whereas the latter is used for the electron microscopy analysis, because it is suitable for sample preparation. The CBD CdS films were prepared by immersing the substrates in an aqueous solution of Cd acetate, thiourea, ammonium acetate, and ammonia, with a pH of 9.5, for 37 min, at 90 °C. The thiourea was the source of S, and the Cd acetate was the source of Cd. The other components had the function of completing the reaction process and keeping the pH at the desired level. The average thickness of the films was 88 nm. For the CSS deposition, the substrate temperature was 475 °C, source temperature was 650 °C, pressure was 10 Torr of He and deposition time was 10 min. The average thickness

*Corresponding author..
E-mail address: helio_moutinho@nrel.gov (H.R. Moutinho).

0040-6090/03/$ - see front matter
doi:10.1016/S0040-6090(03)00646-1

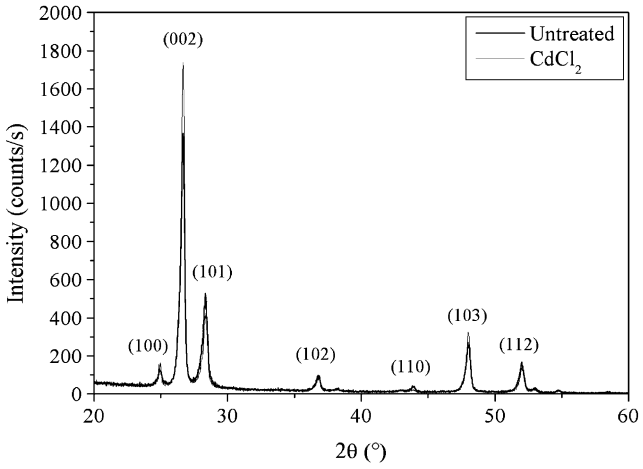

Fig. 1. XRD diffraction patterns for CSS CdS films before and after $CdCl_2$ treatment. Grazing incidence: 0.5°. All peak indices are for the hexagonal structure.

of these films was 115 and 200 nm, for films deposited on SnO_2/glass and SnO_2/Si, respectively. The reason for this divergence is possibly associated with differences in the substrate temperature during deposition of the CdS film. Finally, the samples were treated in $CdCl_2$ vapor at 400 °C, for 5 min, in air. The main advantage of the vapor treatment compared to the traditional dipping process is the simplicity and repeatability of results. Also, it has been shown that this method is more efficient in promoting the recrystallization of CdTe films used in CdTe/CdS solar cells, resulting in more-efficient devices [13].

The films were analyzed with the following techniques: atomic force microscopy (AFM), to study the film morphology, using Si cantilevers and two modes (non-contact, in an Autoprobe LS, from TM Microscopes; and tapping mode, in a Digital Instruments Dimension 3100 AFM; both using active feedback and scan rate of 0.5 Hz); Auger electron spectroscopy (AES), to measure film composition, using a Phi 670 Auger Nanoprobe with field-emission source; transmission electron microscopy (TEM), to analyze the film microstructure, with a Philips CM30 microscope; X-ray diffraction (XRD), to study the microstructure, using grazing incidence mode (GIXRD), in a Scintag X1 diffractometer with Cu target, and Bragg–Brentano configuration.

3. Results

We did not find any major influence of the substrate on the properties of the CdS films. Not even the grain size of the CSS CdS films was influenced by the difference in film thickness for films deposited on different substrates. For this reason, unless explicitly mentioned, we will not make a distinction concerning the substrate used in the following discussion.

Because the CdS films are so thin, normal θ–2θ XRD analysis provided only limited information on the film structure. Therefore, we used grazing-angle incidence, which consists of sending the X-ray beam at very small angles with respect to the film surface. In our case, we used angles varying from 5 to 0.5°. Larger incidence angles probe deeper inside the film, while small angles probe regions close to the surface. In our case, for the observation of the CdS films, the best results were obtained with 0.5°. The GIXRD analysis indicated that the structure of the films is uniform in thickness. Fig. 1 shows XRD patterns for CSS CdS films deposited before and after $CdCl_2$ treatment. The film has a hexagonal structure, and sharp peaks, indicating good crystallinity. As observed in the figure, after the $CdCl_2$ treatment, there are no significant changes in the peak width or position, indicating a similar stress state as before the treatment. For the CBD CdS (Fig. 2), the untreated films have cubic structure, and there is a major change after the $CdCl_2$ treatment. The treated films have a hexagonal structure and sharper peaks. The decrease in peak width is associated with an increase in grain size (see TEM results) and a decrease in the stress within the film. Unfortunately, these two effects could not be separated in the diffraction pattern. This change in crystalline structure has been observed before [14] and is characteristic of the recrystallization process. Recrystallization [15] occurs in strained films as a means to decrease the stress. This process consists of the formation of nuclei at regions of high lattice stress, frequently at grain boundaries; growth of these nuclei, until the old lattice is replaced by a new, low-stress crystalline structure; and, finally, grain growth. The CSS

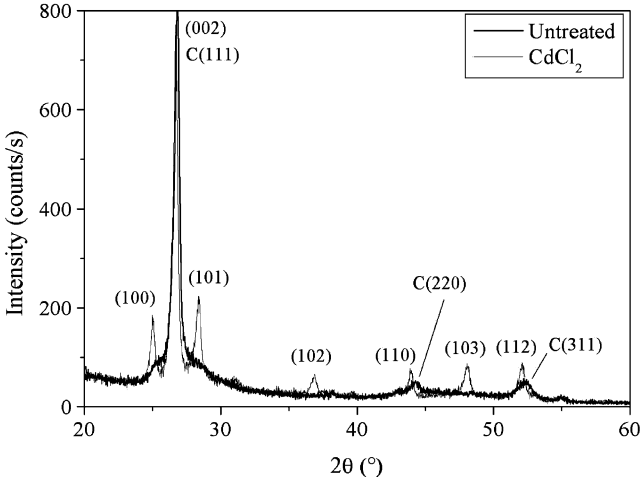

Fig. 2. XRD diffraction patterns for CBD CdS films before and after $CdCl_2$ treatment. Grazing incidence: 0.5°. Indices are for cubic (denoted by a C) and hexagonal structures.

films, grown at a relatively high temperature, already have an energetically favorable orientation and low stress; for this reason, they do not recrystallize. This behavior for CBD and CSS CdS films are very similar to what has been found for CdTe films grown by physical vapor deposition and CSS [16].

The morphology of CBD and CSS films is shown in Fig. 3. No significant changes in morphology occurred after the $CdCl_2$ treatment for either deposition method. There were no features in the AFM images that indicated that the CBD CdS films had been recrystallized during the $CdCl_2$ treatment, as observed in the XRD analysis. Root-mean-square roughness and grain size values are shown in Table 1. For simplicity, we only show data for films grown on SnO_2/Si substrates. However, although the SnO_2 films deposited on glass substrates had a higher roughness, all the observations apply for both substrate structures, including the morphology of the films. We notice that the grain size and roughness values of the CBD films are smaller than the ones of CSS films. The morphology of the SnO_2 films (not shown) is formed by a large variation of grain size, varying from 50 to 250 nm, and influences the morphology of the CBD CdS films. This effect is very important and will be discussed later.

TEM analysis showed that the grain size of the untreated CBD CdS films are on the order of 10 nm, much smaller than the ones observed by AFM. These results were supported by the electron diffraction patterns showed in Fig. 4a. The diffraction rings for the untreated films are continuous, indicating a large number of grains, with different orientations, in the analyzed area. After the treatment, the rings became much less dense, with individual diffraction spots resolved, which is a clear indication of grain growth. In the TEM diffraction patterns, each individual spot in a diffraction ring comes from a different grain. An increase in grain size results in a smaller number of grains diffracting the electron beam, and consequently, a smaller number of spots in the diffraction pattern, making the rings change from continuous to fragmented. These results are important, because they can be related to the XRD data, which showed recrystallization of the CBD CdS films after the $CdCl_2$ treatment. These results indicate that the grains observed in the AFM analysis for the untreated CBD CdS consist of a large number of smaller grains, but this technique lacked the resolution to reveal the subgrain structure. For the CSS CdS films, the grain sizes measured by TEM and AFM were comparable. In Fig. 4a, we notice that most rings for the hexagonal and cubic lattice have similar positions, but the hexagonal phase can be identified by few rings that are not present in the pattern for the untreated film. The $CdCl_2$ treatment

Table 1
CdS films deposited by CSS and CBD on SnO_2/Si substrates, with respective values of roughness and grain size[a]

Deposition method	Sample condition	RMS roughness (nm)	Grain size (nm)
CBD	Untreated	10	81
	$CdCl_2$	9	82
CSS	Untreated	20	142
	$CdCl_2$	17	136
SnO_2/Si		10	127

[a] For comparison purposes, we also show the values of these parameters for the SnO_2/Si substrates.

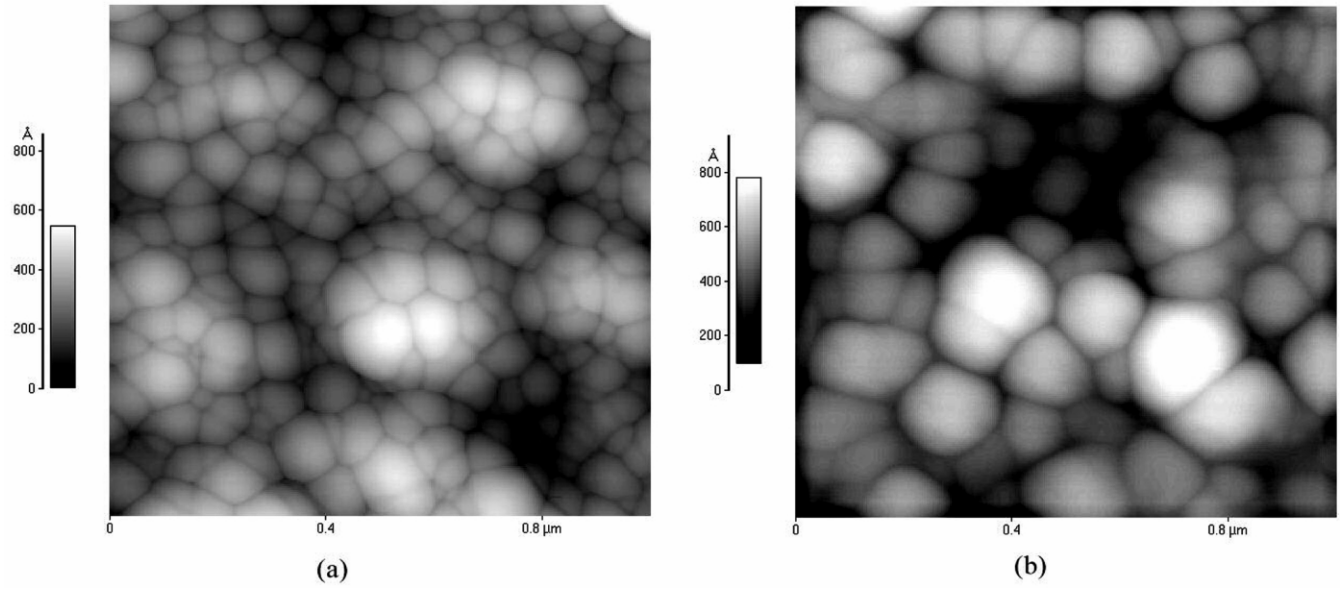

Fig. 3. AFM images of (a) CBD CdS and (b) CSS CdS films.

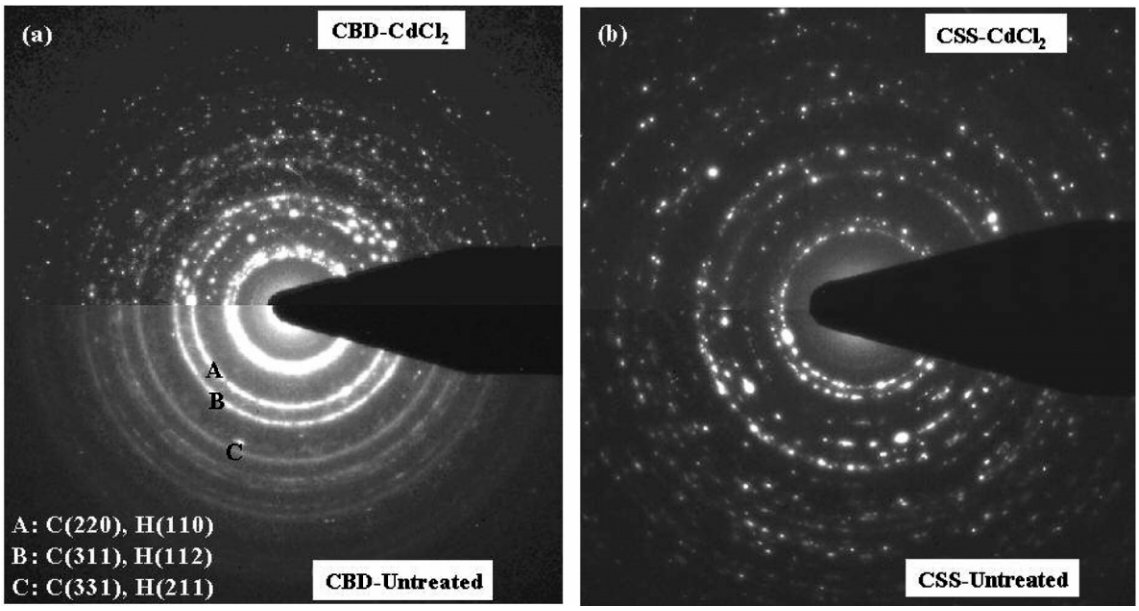

Fig. 4. Electron diffraction patterns for CdS films before and after $CdCl_2$ treatment: (a) CBD CdS, (b) CSS CdS.

did not promote any major changes in the physical properties of the CSS CdS films, as shown in the electron diffraction patterns (Fig. 4b), and observed before in the AFM and XRD analyses. Nevertheless, intragrain stress decreased significantly in these films after the treatment, as indicated by the TEM micrographs shown in Fig. 5. We also observed a significant decrease in the density of planar defects in the CBD CdS films after $CdCl_2$ treatment.

AES depth profiles for untreated CBD and CSS CdS films are shown in Fig. 6. Because of the lack of appropriate standards, our AES results are semiquantitative. We can identify two regions, one with CdS and the other with SnO_2. We also notice that the amount of Cl inside the films are negligible before the $CdCl_2$ treatment, and that although the CSS films are free of oxygen, the CBD films have a significant amount of this element. This characteristic of CBD films is important and will be discussed later. The untreated CSS CdS films had a small quantity of Cl on the surface (Fig.

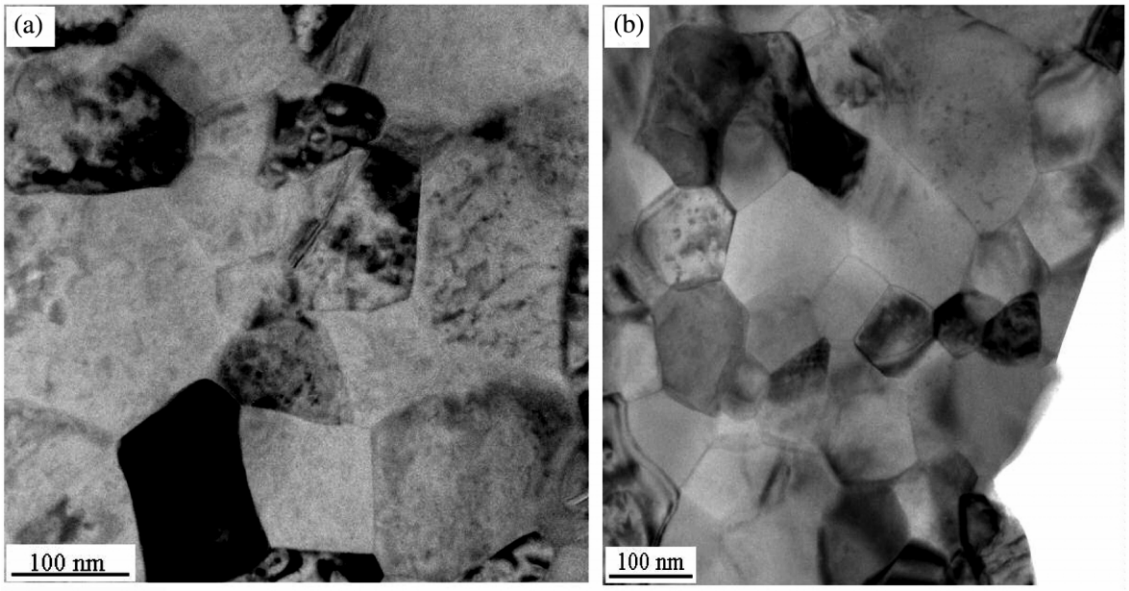

Fig. 5. TEM micrographs of CSS CdS (a) before and (b) after $CdCl_2$ treatment.

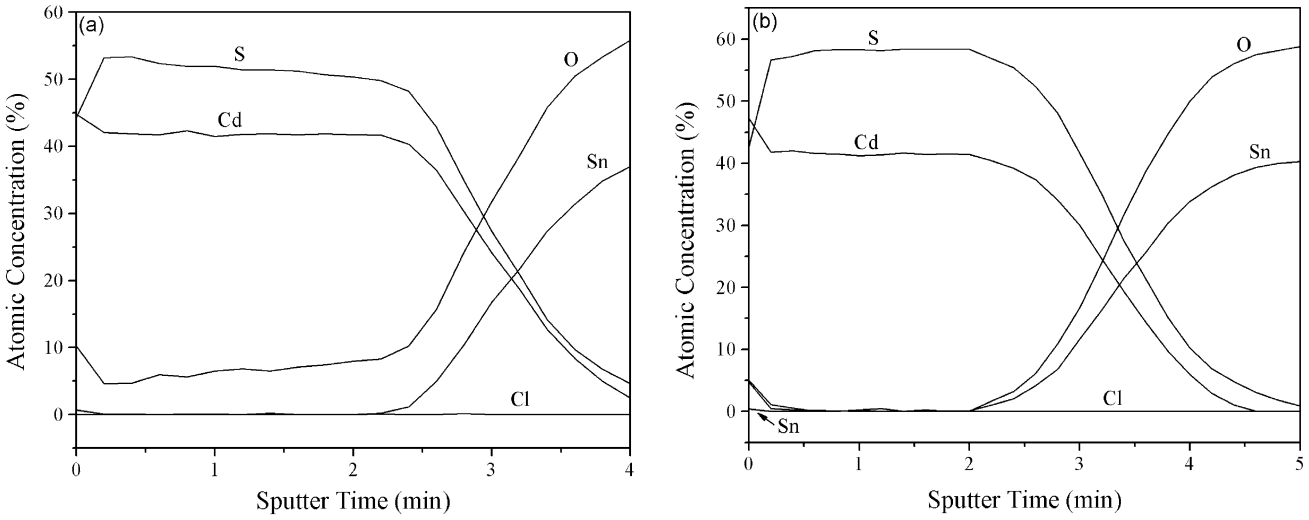

Fig. 6. AES depth profiles of untreated (a) CBD and (b) CSS CdS films.

6b), possibly due to contamination during deposition, because the same vacuum chamber is used for the growth and $CdCl_2$ treatment. After the $CdCl_2$ treatment, there was an increase in the concentration of Cl inside the CBD CdS films, as shown in Fig. 7. These changes were probably due to the high density of defects and to the recrystallization process, which facilitated the diffusion of Cl into the films during the treatment. In contrast, there was no Cl or O in the CSS films after the treatment. This result occurred because these films are grown at relatively high temperatures, probably being denser, and also because they did not undergo recrystallization, which minimized the diffusion of these elements during the treatment.

4. Discussion

The $CdCl_2$ treatment is very important for improving the physical properties of the CBD CdS films through a recrystallization process. The recrystallized material has a much lower density of defects, better crystallinity, and larger grain size. The driving force for the recrystallization process is the high strain energy in the untreated film. CSS CdS films, grown at higher temperatures, have much better crystallinity and, consequently, lower stress; so there is not enough driving force for them to recrystallize during the $CdCl_2$ treatment. Nevertheless, as shown by TEM, the treatment decreases the amount of intragrain strain in these films.

A comparison of the AFM results for CBD CdS and SnO_2 films indicates that the former grows congruently over the latter. The broad undulations observed on the morphology of the CdS films shown in Fig. 3a are caused by large SnO_2 grains. Also, we observe that although the grain size of the CBD CdS film is smaller than that of the SnO_2 film, the roughness for these films is the same. The roughness of the CBD CdS comes mostly from the underlying SnO_2 film, because of the conformal growth. It is important to mention at this point that the small grain size of the untreated CBD CdS film makes congruent growth even easier to obtain. In contrast, the CSS CdS films do not grow congruently, because of their larger grain size and roughness. In Fig. 8, we compare AFM linescans from SnO_2, CBD CdS, and CSS CdS surfaces. The morphology of the CBD CdS is clearly formed by two features. The large features are similar to those observed in the linescan of the SnO_2 film, whereas the smaller features are formed by the CdS grains, which indicates congruent growth. In the case of CSS CdS, the linescan cannot be fitted to the linescan of the SnO_2 film, indicating that congruent growth does not occur. Congruent growth is important

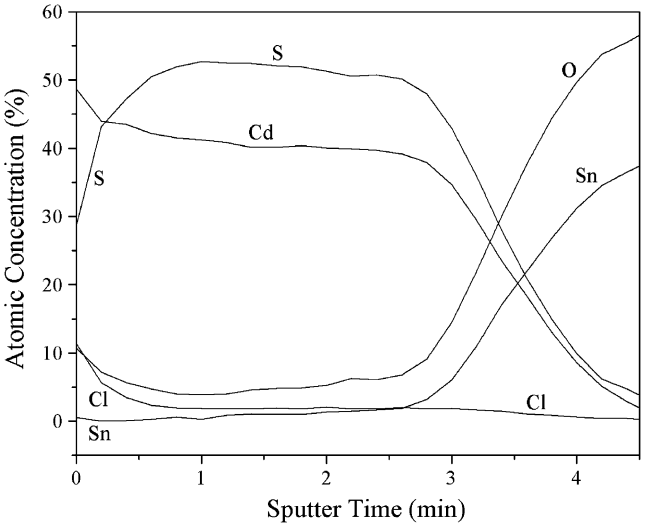

Fig. 7. AES depth profile of a CBD CdS film after $CdCl_2$ treatment.

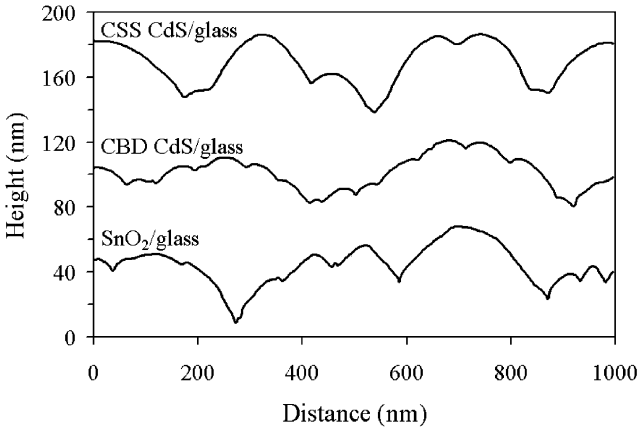

Fig. 8. AFM linescans of the surface of SnO_2 and CBD and CSS CdS films.

because it makes it easier to deposit a uniform CdS film on the SnO_2 with the desired thickness. The uniformity prevents any shunting paths or thick regions that contribute to the series resistance of the solar cell. If there is no congruent growth, the film thickness will vary from point to point. Areas where the CdS film is too thin may result in shunting of the pn-junction, and areas where the film is too thick will result in extra series resistance. So, the congruent growth observed in the CBD CdS films is a very desirable characteristic for application to solar cells.

Another important characteristic of the CBD CdS film is the presence of O in the bulk. It is well known that in CdTe/CdS solar cells, interdiffusion occurs between the CdS and CdTe layers during the $CdCl_2$ treatment [17]. Sulfur diffusion into the CdTe layer is responsible for the thinning of the CdS film and may result in poor performance of the device. Oxygen has been shown to dramatically reduce the diffusion of S into CdTe and Te into CdS at the junction [18,19]. This effect is even more critical if the thickness of the CdS layer is not uniform, as in the case of CSS CdS. Therefore, the O content may be another factor in favor of CBD CdS for use in photovoltaic devices—at least devices with CdTe.

5. Conclusions

CBD CdS films treated in $CdCl_2$ vapor undergo a recrystallization process, which includes grain growth—changing from a cubic to a hexagonal structure—and a decrease in the density of planar defects. In contrast, the $CdCl_2$ treatment does not have such a dramatic effect on the physical properties of CSS CdS films, with only a reduction in intragrain stress observed.

Unlike CSS CdS films, CBD CdS films grow congruently on the SnO_2 substrate structure and have a significant amount of O in their bulk. These two features are probably the reason why solar cells produced with CBD CdS generally result in higher efficiencies than cells prepared with CSS CdS.

Acknowledgments

This work was supported by the US Department of Energy under Contract number DE-AC36-99GO10337.

References

[1] A. Rockett, R.N. Bhattacharya, C. Eberspacher, V. Kapur, S.-H. Wei, Electrochem. Soc. Proc. 99-11 (1999) 232.
[2] A.D. Compaan, J.R. Sites, R.W. Birkmire, C.S. Ferekides, A.L. Fahrenbruch, Electrochem. Soc. Proc. 99–11 (1999) 241.
[3] X. Wu, J.C. Keane, R.G. Dhere, C. DeHart, D.S. Albin, A. Duda, T.A. Gessert, S. Asher, D.H. Levi, and P. Sheldon, Proceedings of the 17th European Photovoltaic Solar Energy Conference, Munich, Germany, October 22–26, 2001, p. 995.
[4] J.S. Ward, K. Ramanathan, F.S. Hasoon, T.J. Coutts, J. Keane, M.A. Contreras, T. Moriarty, R. Noufi, Prog. Photovoltaics: Res. Appl. 10 (2002) 41.
[5] M.A. Contreras, B. Egaas, K. Ramanathan, J. Hiltner, A. Swartzlander, F. Hasoon, R. Noufi, Prog. Photovoltaics: Res. Appl. 7 (1999) 311.
[6] H.R. Moutinho, R.G. Dhere, M.M. Al-Jassim, C. Ballif, D.H. Levi, A.B. Swartzlander, M.R. Young, L.L. Kazmerski, Proceedings of the 28th IEEE Photovoltaic Specialists Conference, Anchorage, U.S.A., September 15-22, 2000, p. 646.
[7] D.H. Rose, F.S. Hasoon, R.G. Dhere, D.S. Albin, R.M. Ribelin, X.S. Li, Y. Mahathongdy, T.A. Gessert, P. Sheldon, Prog. Photovolt: Res. Appl. 7 (1999) 331.
[8] T. Aramoto, S. Kumazawa, H. Higuchi, T. Arita, S. Shibutani, T. Nishio, J. Nakajima, M. Tsuji, A. Hanafusa, T. Hibino, K. Omura, H. Ohyama, M. Murozono, Jpn. J. Appl. Phys. 36 (1997) 6304.
[9] R. Kishore, V. Korapati, H.A. Naseem, W.D. Brown, Proceedings of the 28th IEEE Photovoltaic Specialists Conference, Anchorage, USA, September 15–22, 2000, p. 591.
[10] R.K. Ahrenkiel, D.H. Levi, S. Johnston, Proceedings of the 26th IEEE Photovoltaic Specialists Conference, Anaheim, U.S.A., September 30–October 03, 1997, p. 535.
[11] C. Ferekides, D. Marinksiy, D.L. Morel, Proceedings of the 26th IEEE Photovoltaic Specialists Conference, Anaheim, U.S.A., September 30–October 03, 1997, p. 339.
[12] K. Durose, P.R. Edwards, D.P. Halliday, J. Cryst. Growth 197 (1999) 733.
[13] H.R. Moutinho, R.G. Dhere, C. Ballif, M.M. Al-Jassim, L.L. Kazmerski, J. Vac. Sci. Technol. A 18 (2000) 1599.
[14] J. Touskova, D. Kindl, L. Dobiasova, J. Tousek, Sol. En. Mat. Sol. Cells 53 (1998) 177.
[15] R.E. Reed-Hill, Physical Metallurgy Principles, PWS Publishers, Boston MA, 1973, p. 284.
[16] H.R. Moutinho, M.M. Al-Jassim, D.H. Levi, P.C. Dippo, L.L. Kazmerski, J. Vac. Sci. Technol. A 16 (1998) 1251.
[17] A.J. Chapman, D.W. Lane, K.D. Rogers, M.E. Ozsan, Thin Solid Films 403–404 (2002) 522.
[18] Y. Yan, D. Albin, M.M. Al-Jassim, Appl. Phys. Lett. 78 (2001) 171.
[19] D.S. Albin, Y. Yan, M.M. Al-Jassim, Prog. Photovoltaics: Res. Appl. 10 (2002) 309.